Nano Biomed Eng
2017, 9(2): 107-111. doi: 10.5101/nbe.v9i2.p107-111.

Research Article

Preparation of Upconversion Nanocrystals $NaYF_4$:Yb/Tm with Hydro(solvo)thermal Methods

Feifei Zhao, Dongguang Yin

College of Environmental and Chemical Engineering, Shanghai University, Shanghai 200444, China.

Corresponding author. E-mail: ydg@shu.edu.cn

Received: May 2, 2017; **Accepted:** May 23, 2017; **Published:** May 24, 2017.

Citation: Feifei Zhao, Dongguang Yin, Preparation of Upconversion Nanocrystals $NaYF_4$:Yb/Tm with Hydro(solvo)thermal Methods. *Nano Biomed. Eng.*, 2017, 9(2): 107-111.
DOI: 10.5101/nbe.v9i2.p107-111.

Abstract

A upconversion nanocrystal of $NaYF_4$:Yb/Tm was synthesized successfully by two different methods of solvothermal and hydrothermal, respectively. The properties of the products were characterized and compared. The results showed that the nanocrystal prepared by hydrothermal method exhibited uniform hexagonal phase and large size, while the nanocrystal prepared by solvothermal method displayed high upconversion luminescence (UCL) and small size. The UCL intensity of the nanocrystal from solvothermal method was higher than that of hydrothermal method. This is the first time to systematically compare the performances of the upconversion nanocrystal prepared by solvothermal and hydrothermal methods, which provides some new insight into the preparation of upconversion nanomaterials with intense UCL and controllable morphology.

Keywords: $NaYF_4$; $NaLuF_4$ and $NaGdF_4$-based upconversion nanocrystals; Synthesis; Hydro(solvo)thermal methods; Upconversion luminescence

Introduction

Recently, rare earth upconversion nanocrystals (UCNs) have attracted many attentions due to their unique and attractive properties. In comparison with other fluorescent materials such as organic dyes and quantum dots, UCNs exhibit many advantages such as high photochemical stability, sharp emission peaks, large anti-stokes shifts, low toxicity and long life-time [1-13]. In addition, high penetration depth and absence of autofluorescence make them ideal materials for biological labeling and *in-vivo* imaging [14-19]. To date, a lot of fluoride-based host matrixs and UCNs have been developed. Among these materials, $NaYF_4$ is regarded as an excellent host matrix due to its low phonon energy and high refractive index, and $NaYF_4$:Yb, Tm is well-known as one of the efficient UCNs [20-23].

At present, many approaches for preparing lanthanide-doped UCNs have been developed, such as hydrothermal, solvothermal, thermal decomposition, and ionic liquids methods [24]. Among these approaches, thermal decomposition of trifluoroacetate precursors has the advantages of controllable size and morphology. However, it exhibits drawbacks of rigorous reaction conditions, hazardous precursors and coordinating solvents [25-27]. Ionic liquids method has the merit of mild reaction condition and user-friendly regents, but exhibits drawbacks of poor shape-control and broad size distribution [14].

Usually, hydrothermal and solvothermal are considered as popular and effective methods, which own the merits of facile, mild reaction condition, no toxicity, narrow size distribution and modulatable shape [28-30]. However, no study has concretely compared the performances of the upconversion nanocrystal prepared by solvothermal and hydrothermal methods. In this study, we concretely compared the performances of the upconversion nanocrystal $NaYF_4$:Yb, Tm prepared by the two different methods. This work could provide new insight into the preparation of upconversion nanomaterials with strong upconversion luminescence (UCL) and uniform morphology.

Experimental

Materials

Rare earth oxides Y_2O_3 (99.999%), Yb_2O_3 (99.999%) and Tm_2O_3 (99.999%) were purchased from Shanghai Yuelong New Materials Co. Ltd. Oleic acid (OA) (> 90%) and 1-octadecene (> 90%) were purchased from Sigma-Aldrich. NaOH, NH_4F, NaF, sodium citrate, hydrochloric acid, ethanol, methanol and cyclohexane were supplied by Sinopharm Chemical Reagent Co., Ltd. (Shanghai). YCl_3 and $YbCl_3$ were prepared by dissolving their corresponding metal oxides in hydrochloric acid at elevated temperature.

Synthesis of $NaYF_4$:Yb/Tm by solvothermal method

To synthesize $NaYF_4$:Yb/Tm, 0.78 mmol of YCl_3, 0.20 mmol of $YbCl_3$, and 0.02 mmol of $TmCl_3$ were mixed with 6 mL oleic acid (OA) and 15 mL octadecene (ODE) in 50 mL three-necked flask. The solution was heated to 160 °C for 30 min and then cooled to room temperature. Subsequently, 10 mL methanol solution containing NaOH (4 mmol) and NH_4F (2.5 mmol) were slowly added into the flask and kept for 30 min. The solution was heated to 100 °C and kept for 30 min to remove methanol and water, then heated to 300 °C under nitrogen atmosphere and kept for 1 h. After the solution was allowed to cool down to room temperature, nanocrystals were precipitated from the solution with ethanol, and collected after centrifuging and washing with ethanol/water (1:1 v/v) for three times.

Synthesis of $NaYF_4$:Yb/Tm by hydrothermal method

In a typical synthesis, 0.78 mmol of YCl_3, 0.20 mmol of $YbCl_3$, and 0.02 mmol of $TmCl_3$ were mixed with 10 mL de-ionized water in flask. Then 20 mL of aqueous solution containing 2 mmol sodium citrate were added to the flask to form metal citrate complex. After vigorous stirring for 30 min, 30 mL of aqueous solution containing 25 mmol of NaF was introduced into the above solution. Vigorous stirring was maintained for another 60 min. Then, the mixing solution was transferred into a Teflon bottle held in a stainless steel autoclave, sealed and maintained at 180 °C for 24 h. As the autoclave was cooled to room temperature naturally, the precipitates were separated by centrifugation, washed with ethanol and deionized water in sequence, and then dried in air at 60 °C. Finally, the desired products was obtained.

Characterization

Scanning electron microscopy (SEM) images were measured with a JSM-6700F electron microscope. X-ray powder diffraction (XRD) measurements were performed on a Rigaku D/max-2500 X-ray diffractometer using Cu Kα radiation. Transmission electron microscopy (TEM) analyses were performed on a JEOL JEM-2010F electron microscope operating at 200 kV. The upconversion luminescence emission spectra were recorded with an Edinburgh LFS-920 fluorescence spectrometer by using an external 0-2 W adjustable laser (980 nm, Beijing Hi-Tech Optoelectronic Co., China) as the excitation source instead of the Xenon source in the spectrophotometer.

Results and Discussion

Structure and morphology of the nanocrystals

The phase compositions of the as-prepared samples were detected by the powder XRD. As shown in Fig. 1, the diffraction peaks of the $NaYF_4$:Yb/Tm prepared by solvothermal method could be indexed

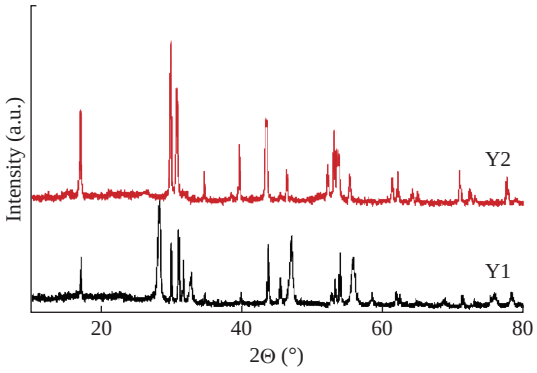

Fig. 1 XRD patterns of the $NaYF_4$:Yb/Tm prepared by solvothermal method (Y1) and hydrothermal method (Y2), respectively.

as mixed phase crystals including cubic (JCPDS: 77-2042) and hexagonal (JCPDS: 16-0334) phases [29], while the diffraction peaks of the product prepared by hydrothermal method could be indexed as pure hexagonal phase crystals.

TEM and SEM were used to observe the morphology and size of the nanocrystals. As shown in Fig. 2, $NaYF_4$:Yb/Tm prepared by solvothermal method displayed mixed phase structures, including cubic and hexagonal phases, with average diameter of about 25 nm. Whereas $NaYF_4$:Yb/Tm prepared by hydrothermal method exhibited pure hexagonal phase structure, with average diameter of about 500 nm. These results agree well with the XRD results, revealing that hydrothermal method is facile to generate uniform pure hexagonal-phase nanocrystals with relatively large sizes, while the solvothermal method is facile to generate mixed phase nanocrystals with relatively small sizes.

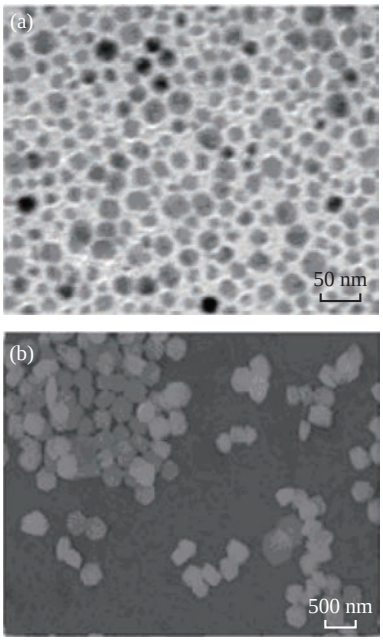

Fig. 2 (a) TEM and **(b)** SEM images of $NaYF_4$:Yb/Tm prepared by solvothermal and hydrothermal methods, resepctively.

Upconversion luminescence properties of the nanocrystals

The upconversion luminescenne properties of the as-prepared nanocrystals were investigated. As shown in Fig. 3, upon continuous-wave excitation at 980 nm, nanocrystals prepared by solvothermal and hydrothermal methods exhibited similar UCL spectra with an excellent 800 nm near-infrared (NIR) UCL and an weak emission band at 700 nm. The emission band peaked at 700 nm was caused by $^3F_3$-$^3H_6$ transitions

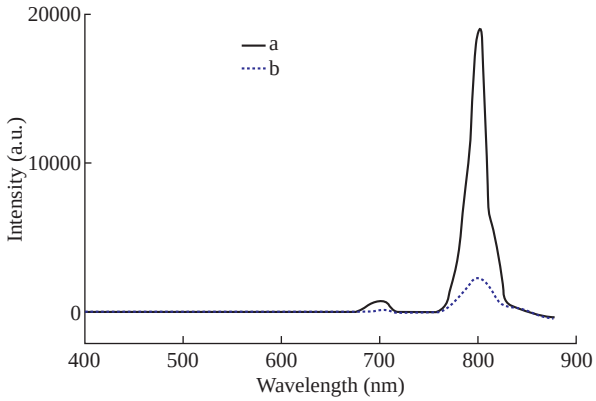

Fig. 3 Upconversion luminescent spectra of $NaYF_4$:Yb/Tm prepared by **(a)** solvothermal method and **(b)** hydrothermal method, respectively.

of Tm^{3+}, while the predominant NIR emission peak at 800 nm was caused by $^3H_4$-$^3H_6$ transition, respectively [22, 24]. The UCL intensities of the prepared samples were measured at the same concentration of 1.0 mg/mL in cyclohexane. Interestingly, it was found that the UCL intensity of the product prepared by solvothermal method was much higher than that by hydrothermal method, though the size of the product by solvothermal method was much smaller than that of hydrothermal counterpart.

The difference between the UCL intensities of the nanocrystals prepared by solvothermal method and hydrothermal method are supposed to be mainly due to the differences of capping reagent and the reaction temperature involving in the two synthetic methods. In contrast with citric acid, OA is considered as a more powerful capping reagent which can eliminate the surface defects of the nanocrystals efficiently, leading the nanocrystals to exhibiting a higher upconversion luminescence [31]. The carboxyl group of the citric acid molecule is a high energy vibration group with a high energy vibration mode, which can cause a quench of upconversion luminescence of the Ln^{3+} through a multi-phonon relaxation process [32, 33]. The reaction temperature in solvethermal method is higher than that of hydrothermal method. A high reaction temperature favors the generation of high crystallinity and the elimination of surface defects of the nanocrystals, resulting in a high upconversion luminescence [34-36].

Conclusions

In summary, upconversion nanocrystal $NaYF_4$:Yb/Tm was synthesized successfully by hydrothermal and solvothermal methods respectively. The properties of

the products prepared by the two different synthesis methods were systematically compared. The results show that the UCL intensity of the nanocrystal prepared by solvothermal method was higher than that by hydrothermal method. Under the experimental conditions, the hydrothermal method made the nanocrystal exhibit a uniform pure hexagonal phase and large sizes, while the solvothermal method made the nanocrystals display a high UCL intensity and small sizes.

Acknowledgments

The authors acknowledge that this article was funded partially by the National Natural Science Foundation of China (No. 21271126), National 973 Program (No. 2010CB933901) and Shanghai Leading Academic Discipline Project (No. S30109).

References

[1] Y.J. Zhao, X.W. Zhao, and Z.Z. Gu, Photonic crystals in bioassays. *Advanced Functional Materials*, 2010, 20: 2970-2988.

[2] Y.J. Zhao, X.W. Zhao, J. Hu, et al., Encoded porous beads for label-free multiplex detection of tumor markers. *Advanced Materials*, 2009, 21: 569-572.

[3] F. Wang, C. Ma, X. Zeng, et al., Chemiluminescence molecular detection of sequence-specific HBV-DNA using magnetic nanoparticles. *Journal of Biomedical Nanotechnology*, 2012, 8: 786-790.

[4] T. Xiong, Y.J. Li, F.G. Ni, et al., Monitoring of bystander effect of herpes simplex virus thymidine kinase/acyclovir system using fluorescence resonance energy transfer technique. *Journal of Biomedical Nanotechnology*, 2012, 8: 74-79.

[5] M. Zuzana, R. Alessandra, F. Lise, et al., Safety assessment of nanoparticles cytotoxicity and genotoxicity of metal nanoparticles in vitro. *Journal of Biomedical Nanotechnology*, 2011, 7: 20-21.

[6] M.L. Jugan, S. Barillet, A. Simon-Deckers, et al., Cytotoxic and genotoxic impact of TiO_2 nanoparticles on A549 cells. *Journal of Biomedical Nanotechnology*, 2011, 7: 22-23.

[7] R. Wahab, Y.B. Yang, A. Umar, et al., Platinum quantum dots and their cytotoxic effect towards myoblast cancer cells (C_2C_{12}). *Journal of Biomedical Nanotechnology*, 2012, 8: 424-431.

[8] A. Babu, K. Jeyasubramanian, P. Gunasekaran, et al., Gelatin nanocarrier enables efficient delivery and phototoxicity of hypocrellin B against a mice tumour model. *Journal of Biomedical Nanotechnology*, 2012, 8: 43-56.

[9] Y.J. Zhao, H.C. Shum, H.S. Chen, et al., Microfluidic generation of multifunctional quantum dot barcode particles. *Journal of the American Chemical Society*, 2011, 133: 8790-8793.

[10] R.D. Umrani, K.M. Paknikar, Ayurvedic medicine zinc bhasma: Physicochemical evaluation, anti-diabetic activity and safety assessment. *Journal of Biomedical Nanotechnology*, 2011, 7: 148-149.

[11] F.P. Navarro, M. Berger, S. Guillermet, et al., Lipid nanoparticle vectorization of indocyanine green improves fluorescence imaging for tumor diagnosis and lymph node resection. *Journal of Biomedical Nanotechnology*, 2012, 8: 730-741.

[12] S. Li, H.N. Liu, Y.Y. Jia, et al., A novel SNPs detection method based on gold magnetic nanoparticles array and single base extension. *Theranostics*, 2012, 2: 967-975.

[13] N.Y. He, F. Wang, C. Ma, et al., Chemiluminescence analysis for HBV-DNA hybridization detection with magnetic nanoparticles based DNA extraction from positive whole blood samples. *Journal of Biomedical Nanotechnology*, 2013, 9: 267-273.

[14] J.C.G. Bünzli, Lanthanide luminescence for biomedical analyses and imaging. *Chemical Reviews*, 2010, 110: 2729-2755.

[15] J. Ryu, H.Y. Park, K. Kim, et al., Facile synthesis of ultrasmall and hexagonal $NaGdF_4$: Yb^{3+}, Er^{3+} nanoparticles with magnetic and upconversion imaging properties. *The Journal of Physical Chemistry C*, 2010, 114: 21077-21082.

[16] Z.Q. Li, H.S. Qian, Y. Hu, et al., Seed-mediated synthesis of $NaYF_4$:Yb, Er/$NaGdF_4$ nanocrystals with improved upconversion fluorescence and MR relaxivity. *Nanotechnology*, 2010, 21: 125602-125607.

[17] C.X. Li, J. Lin, Rare earth fluoride nano-/microcrystals: synthesis, surface modification and application. *Journal of Materials Chemistry*, 2010, 20: 6831-6847.

[18] J. Shen, L.D. Sun, and C.H. Yan, Luminescent rare earth nanomaterials for bioprobe applications. *Dalton Transactions*, 2008, 42: 5687-5697.

[19] P. Zhang, W. Steelant, M. Kumar, et al., Versatile photosensitizers for photodynamic therapy at infrared excitation. *Journal of the American Chemical Society*, 2007, 129: 4526-4527.

[20] J. Zhou, Z. Liu, and F.Y. Li, Upconversion nanophosphors for small-animal imaging. *Chemical Society Reviews*, 2012, 41: 1323-1349.

[21] H. Kobayashi, M. Ogawa, R. Alford, et al., New strategies for fluorescent probe design in medical diagnostic imaging. *Chemical Reviews*, 2010, 110: 2620-2640.

[22] P. Tallury, S. Santra, P. Sharma, et al., Fluorescent and paramagnetic chitosan nanoparticles that exhibit high magnetic resonance relaxivity: Synthesis, characterization and in vitro studies. *Journal of Biomedical Nanotechnology*, 2011, 7: 724-729.

[23] S. Schietinger, T. Aichele, H.Q. Wang, et al., Plasmon-enhanced upconversion in single $NaYF_4$: Yb^{3+}/Er^{3+} codoped nanocrystals. *Nano Letters*, 2010, 10: 134-138.

[24] H.T. Wong, H.L.W. Chan, and J.H. Hao, Towards pure near-infrared to near-infrared upconversion of multifunctional GdF_3:Yb^{3+}, Tm^{3+} nanoparticles. *Optics Express*, 2010, 18: 6123-6130.

[25] B. Sitharaman, L.J. Wilson, Gadofullerenes and gadonanotubes: A new paradigm for high-performance magnetic resonance imaging contrast agent probes. *Journal of Biomedical Nanotechnology*, 2007, 3: 342-352.

[26] S. Tiwari, Y.M. Tan, and M. Amiji, Preparation and in vitro characterization of multifunctional nanoemulsions for simultaneous MR imaging and targeted drug delivery. *Journal of Biomedical Nanotechnology*, 2006, 2: 217-224.

[27] K. *König*, Multiphoton microscopy in life sciences. *Journal of Microscopy*, 2000, 200: 83-104.

[28] X.F. Yu, L.D. Chen, M. Li, et al., Highly efficient fluorescence of NdF_3/SiO_2 core/shell nanoparticles and the applications for in vivo NIR detection. *Advanced Materials*, 2008, 20: 4118-4123.

[29] F. Wang, Y. Han, C.S. Lim, et al., Simultaneous phase and size control of upconversion nanocrystals through lanthanide doping. *Nature*, 2010, 463:1061-1065.

[30] J. Zhou, M.X. Yu, Y. Sun, et al., Fluorine-18-labeled $Gd^{3+}/Yb^{3+}/Er^{3+}$ co-doped $NaYF_4$ nanophosphors for multimodality PET/MR/UCL imaging. *Biomaterials*, 2011, 32: 1148-1156.

[31] C.H. Liu, J. Sun, H. Wang, et al., Size and morphology controllable synthesis of oil-dispersible LaF_3: Yb, Er upconversion fluorescent nanocrystals via a solid-liquid two-phase approach. *Scripta Materialia*, 2008, 58: 89-92.

[32] J.W. Zhao, Y.J. Sun, X.G. Kong, et al., Controlled synthesis, formation mechanism, and great enhancement of red upconversion luminescence of $NaYF_4$: Yb^{3+}, Er^{3+} nanocrystals/submicroplates at low doping level. *The Journal of Physical Chemistry B*, 2008, 112: 15666-15672.

[33] X.M. Liu, J.W. Zhao, Y.J. Sun, et al., Ionothermal synthesis of hexagonal-phase $NaYF_4$: Yb^{3+}, Er^{3+}/Tm^{3+} upconversion nanophosphors. *Chemical Communications*, 2009, 43: 6628-6630.

[34] F. Shi, J.S. Wang, X.S. Zhai, et al., Facile synthesis of β-$NaLuF_4$:Yb/Tm hexagonal nanoplates with intense ultraviolet upconversion luminescence. *Cryst Eng Comm*, 2011, 13: 3782-3787.

[35] X.G. Peng, An essay on synthetic chemistry of colloidal nanocrystals. *Nano Research*, 2009, 2: 425-447.

[36] M.L. Steigrwald, L.E. Brus, Semiconductor crystallites: a class of large molecules. *Accounts of Chemical Research*, 1990, 23: 183-188.